International Core Journal of Engineering Volume 11 Issue 4, 2025
ISSN: 2414-1895 DOI: 10.6919/ICJE.202504_11(4).0028

Red Luminescent Material based on $NaLi_3SiO_4$ Matrix Doped with Mn^{2+} and its Site Occupancy and Luminescence Properties

Qiue Chen*

School of Physics and Optoelectronic Engineering, Guangdong University of Technology, Guangzhou 510000, China

*Correspondence Author: Qiue Chen

Abstract

This paper reports a red luminescent material based on a $NaLi_3SiO_4$ matrix doped with Mn^{2+} and explores its preparation method and optical properties. The results indicate that Mn^{2+} ions occupy the octahedral coordination site of Na^+ ions and exhibit red light emission at 677 nm to 698 nm under 428 nm excitation. As the Mn^{2+} doping concentration increases, the emission intensity is enhanced, and the emission wavelength shifts to the red region. The material is synthesized using a high-temperature solid-phase method, sintered at 850°C under a reducing atmosphere for 4 hours. This material exhibits excellent chemical stability and optical properties, making it promising for applications in LED lighting and display technology.

Keywords

Mn^{2+} Doping; Red Luminescent Material; Optical Properties; UCr_4C_4-type Silicate.

1. Introduction

As a key component of optoelectronic technology, luminescent materials have been widely used in display technology, lasers, solar cells, optical communication, sensors and biomedical imaging. In recent years, with the rapid development of optoelectronic devices, the market demand for high-performance luminous materials has increased significantly. Among many photoelectric materials, rare earth metal ions and transition metal ions have become the focus of research because of their unique electronic structures and excellent luminescence properties.[1]

Mn^{2+} is a transition metal ion that plays a significant role in modern lighting and display technologies. The $3d^5$ electronic configuration of Mn^{2+} determines its spectral characteristics, with its luminescence primarily arising from transitions from the $^6A_1$ (ground state) to $^4T_1$ and $^4T_2$ (excited states)[2]. The emission spectrum of Mn^{2+} is largely influenced by the crystal field strength, as different host crystal fields alter the splitting of energy levels in the excited states, thereby tuning the color of the emitted light. In a weak crystal field environment, the emission typically appears as green light (~520 nm), while in a strong crystal field, the emission tends to shift toward orange-red light (~600 nm). In recent years, Mn^{2+}-activated narrow-band green phosphors have been continuously developed, with their full width at half maximum (FWHM) gradually narrowed. For example, materials such as oxynitride γ-AlON[3], $MgAl_2O_4:Mn^{2+}$[4], $BaZnAl_{10}O_{17}:Mn^{2+}$[5], and $ZnAl_2O_4:Mn^{2+}$[6] have demonstrated excellent performance. Research by Lei et al. also revealed that Mn^{2+}-doped tetrahedral AlN phosphors can emit red light, which significantly differs from the luminescence behavior observed in oxide hosts[7]. This phenomenon is primarily attributed to two reasons: first, the d-orbital electron cloud rearrangement effect in nitride hosts shifts the energy level center of Mn^{2+} toward lower energy; second, the high charge of N^{3-} enhances the crystal field strength around Mn^{2+}[2]. Although the stringent synthesis conditions of nitride compounds result in higher costs, Mn^{2+} is more cost-effective

ISSN: 2414-1895 DOI: 10.6919/ICJE.202504_11(4).0028

compared to rare-earth ions. The transitions of Mn^{2+} are spin-forbidden (d-d transitions), resulting in relatively long fluorescence lifetimes (typically on the order of milliseconds). Additionally, rare-earth ion-doped systems face significant challenges in achieving long-wavelength emission properties, creating more opportunities for the development of Mn^{2+}-based materials.

$NaLi_3SiO_4$ as a UCr_4C_4-type silicate host material, possesses excellent chemical stability, a low thermal expansion coefficient, and favorable optical properties, making it an ideal host for luminescent materials[8]. Doping with transition metal ions such as Mn^{2+} in the $NaLi_3SiO_4$ host can significantly enhance luminescence intensity and tune the emission wavelength. Moreover, its unique crystal structure provides a suitable coordination environment for the incorporation of various ions, thereby further improving the efficiency of energy transfer.

In this work, we designed and synthesized Mn^{2+}-doped $NaLi_3SiO_4$ luminescent materials, refined their structures based on high-quality XRD powder diffraction data, studied the structure, phase purity, and Mn^{2+} ion site occupancy properties of the synthesized samples. Through X-ray absorption spectroscopy tests, we analyzed the valence states of Mn^{2+} ions and the evolution of local coordination environments. We conducted PL spectroscopy tests on doped samples to study the spectral level structure of the samples at low temperatures, analyzed the effects of doping concentration and temperature on the luminescent properties of the samples, and explored the crystal field and electron-phonon coupling effects on Mn^{2+} ions.

2. Experimental Section

materials and preparation. The $Na_{1-x}Li_3SiO_4$: xMn^{2+} (x=1%,5%,10%) samples were prepared using a high-temperature solid-state reaction method. Raw materials, including Na_2CO_3 (Aladdin, 99.99%), $LiCO_3$ (Aladdin, 99.99%), SiO_2 (Aladdin, 99.99%), and $MnCO_3$ (Aladdin, 99.99%), were weighed according to the stoichiometric ratios. The raw materials were thoroughly mixed in an agate mortar and ground uniformly for 20 minutes using 10mL of ethanol. The mixture was then dried under a red lamp until completely dry. Subsequently, the mixture was sintered at 850°C for 4 hours in a N_2-H_2 reducing atmosphere. After cooling to room temperature, the samples were ground into fine powders for further characterization

Characterization. The X-ray diffraction (XRD) data of the samples were measured in the range of 10° to 80° using an X-ray diffractometer to investigate the phase purity and structural changes. The photoluminescence (PL) spectra and luminescence decay curves were measured under 428 nm excitation in the range of 500–800 nm using a combined spectrometer. Additionally, the excitation spectrum was monitored at the emission wavelength of 677 nm. A xenon lamp was used as the excitation source for steady-state luminescence measurements, and a nanosecond pulsed light-emitting diode (LED) was employed to measure the luminescence decay curves of the samples.

3. Result and Discussion

3.1 Crystal Structure Analyses

$NaLi_3SiO_4$ belongs to the UCr_4C_4-type oxides and possesses a highly symmetric body-centered tetragonal structure with the space group $I4_1/a$ (88). Its crystal structure is illustrated in Fig1. The unit cell parameters are a = 10.78 (1) Å, c = 12.63 (1) Å, V = 1468 $Å^3$, and Z = 16. The structural framework of this compound contains two types of tetragonal channels running along the c-axis, which are formed by SiO_4 and LiO_4 tetrahedra. Among these, Channel A has a longer cross-sectional diagonal (~4.40 Å), while Channel B has a shorter one (~4.14 Å). In the structure, the single Na^+ site is located within Channel A, coordinated with eight oxygen atoms, with an effective ionic radius of ~1.18 Å[9]. The site symmetry is C_1, and the average bond length is ~2.61 Å.

ISSN: 2414-1895 DOI: 10.6919/ICJE.202504_11(4).0028

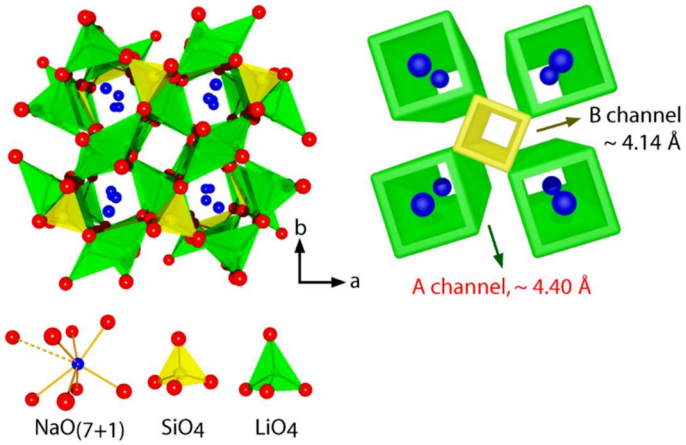

Fig. 1 Crystal structure of $NaLi_3SiO_4$

The doping of Mn^{2+} can be further determined by the difference in ionic radii between the doping ion and the substituting ion[10]:

$$D_r = \frac{R_m(CN) - R_d(CN)}{R_m(CN)} \quad (1)$$

Here, D_r represents the percentage difference in radii, CN is the coordination number, and $R_m\ (CN)$ and $R_d\ (CN)$ denote the radii of the host cation and the doped ion, respectively. Generally, an acceptable D_r value should be less than 0.3. For the positions of Na^+ (1.18 Å) and Li^+ (0.59 Å), the effective ionic radius of Mn^{2+} in an eight-coordinated environment is approximately 0.96 Å. The calculated D_r values are 0.19 and 0.62, respectively. This indicates that in the $NaLi_3SiO_4$ host lattice, Mn^{2+} will preferentially substitute the Na^+ sites. The extra positive charge generated by this doping is theoretically compensated by a nearby negatively charged Na^+ vacancy V' within the channels[11].

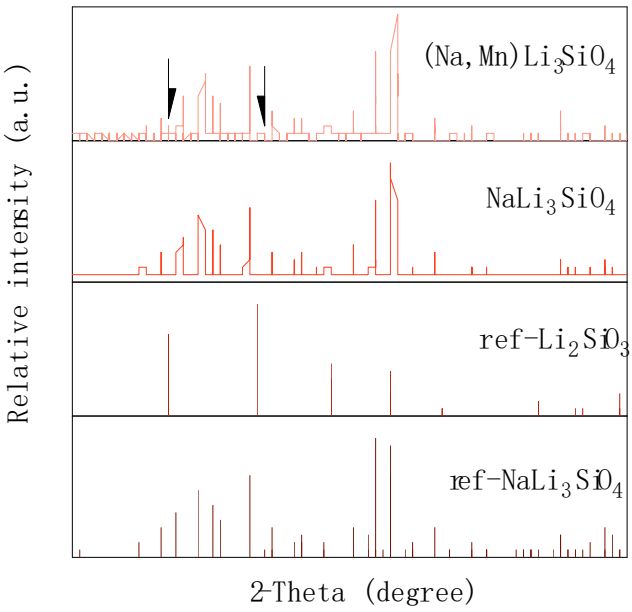

Fig. 2 XRD pattern of $NaLi_3SiO_4$ matrix and its doped sample

ISSN: 2414-1895 DOI: 10.6919/ICJE.202504_11(4).0028

Fig.2 shows the XRD pattern of $NaLi_3SiO_4$. In the XRD spectra of the doped samples, weak diffraction peaks are observed at approximately 19° and 27°. By comparing with standard reference cards, we attribute these diffraction peaks to a small amount of Li_2SiO_3 impurity in the synthesized samples. Considering that the larger ionic size of the doped Mn^{2+} ions prevent them from entering the Li_2SiO_3 impurity phase, the presence of Li_2SiO_3 in the doped samples does not affect the luminescent properties of the main phase, (Na, Mn) Li_3SiO_4.

3.2 Optical Properties

Photoluminescence (PL) spectroscopy characterization was performed on the doped samples $Na_{1-x}Li_3SiO_4$: x Mn^{2+} (x = 1%, 5%, 10%). Fig3 shows the normalized excitation (λ_{em} = 677 nm) and emission (λ_{ex} = 428, 441 nm) spectra of the $Na_{0.99}$ Li_3SiO_4: 1% Mn^{2+} sample at room temperature. When monitoring the 677 nm emission, the excitation spectrum of the sample exhibits six distinct excitation peaks at wavelengths of approximately ~360 nm, ~384 nm, ~428 nm, ~442 nm, ~472 nm, and ~514 nm. These excitation peaks originate from the d-d transitions of Mn^{2+} ions from the ground state $^6A_1$ (^6S) to the excited states, specifically the ^4E (^4D), $^4T_2$ (^4D), ^4E, $^4A_1$ (^4G), $^4T_2$ (^4G), and $^4T_1$ (^4G) levels[12]. Among these, the excitation peak at ~428 nm [$^6A_1$ (^6S) → ^4E, $^4A_1$ (^4G)] exhibits the highest intensity. Under 428 nm excitation, the sample displays an emission band with a peak at ~677 nm. This long-wavelength red emission from Mn^{2+} ions is consistent with the structural analysis of its occupancy in the eight-coordinated Na^+ site. The full width at half maximum (FWHM) of this emission peak is ~2787 cm^{-1} (~130 nm), attributed to the $^4T_1$ (^4G) → $^6A_1$ (^6S) transition. From this, the Stokes shift of the Mn^{2+} ion emission is calculated to be ~4684 cm^{-1}.

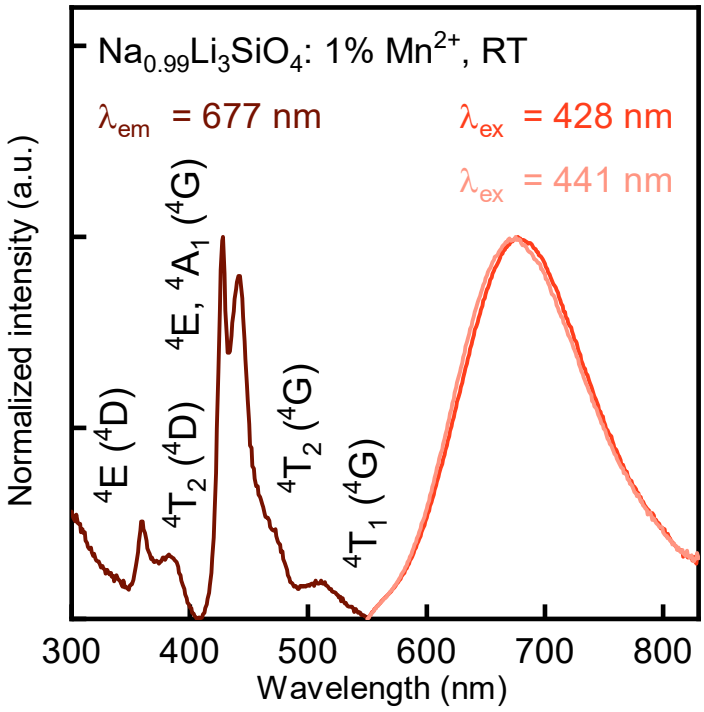

Fig. 3 The normalized excitation (λ_{em} = 677 nm) and emission (λ_{ex} = 428, 441 nm) spectra of the $Na_{0.99}$ Li_3SiO_4: 1% Mn^{2+} sample at room temperature, with the highest intensity normalized.

Additionally, as shown in Fig. 3, the emission spectrum of the sample under ~441 nm excitation overlaps with that under ~428 nm excitation, indicating that there is only one Mn^{2+} ion emission center in the sample. This is consistent with the earlier analysis that there is only one Na^+ ion site available for Mn^{2+} ion substitution in the host matrix. Finally, the sample exhibits red emission under 365 nm ultraviolet light (see Fig. 4).

ISSN: 2414-1895 DOI: 10.6919/ICJE.202504_11(4).0028

Fig. 4 Luminescence photograph of $Na_{0.99}Li_3SiO_4$: 1% Mn^{2+} sample under UV irradiation at 365 nm

The CIE1931 chromaticity coordinates were measured to evaluate the color properties of the luminescent materials. The samples' emission was mapped in the CIE 1931 chromaticity diagram, with coordinates determined at (0.656, 0.344) for 1% Mn^{2+} doping, (0.660, 0.339) for 5% doping, and (0.680, 0.310) for 10% doping. The chromaticity coordinates demonstrated a red-shift trend with increasing Mn^{2+} concentration, which aligns with the spectral shift observed in fluorescence measurements. The color purity was also calculated, indicating that the samples exhibit a deep red emission suitable for LED and display applications. Compared to conventional red phosphors, the Mn^{2+}-doped NaLi3SiO4 materials show superior chromaticity stability and minimal color degradation under prolonged operation.

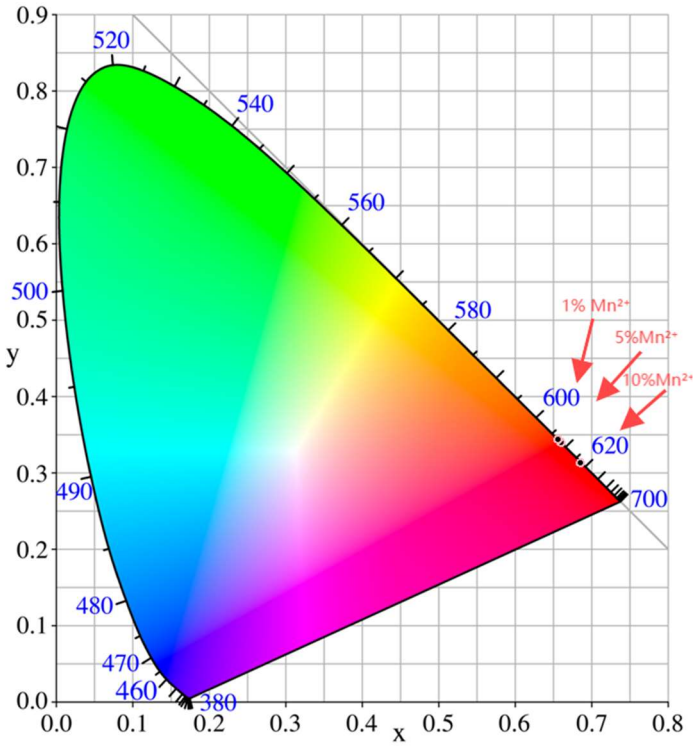

Fig. 5 CIE coordinates of $Na_{0.99}Li_3SiO_4$:1%Mn^{2+},5%Mn^{2+},10%Mn^{2+}

Fig. 6 shows the concentration-dependent excitation (a), emission (b) spectra, and lifetime decay curves (c) of the Na_{1-x} Li_3SiO_4: x Mn^{2+} (x = 1%, 5%, 10%) samples at room temperature. From Fig 6 (a), it can be observed that as the doping concentration increases, the excitation spectra of the Mn^{2+} ions almost overlap, with no change in the wavelength positions of the corresponding excitation

ISSN: 2414-1895 DOI: 10.6919/ICJE.202504_11(4).0028

energy levels. Under 428 nm excitation, the intensity of the emission band in the emission spectra [see Fig6 (b)] increases with higher doping concentrations, but the peak wavelength shifts from ~677 nm to ~692 nm and further to ~698 nm. This indicates that within the concentration range designed in this experiment (1% ~ 10%), the Mn^{2+} ion emission does not exhibit concentration quenching in terms of emission intensity. Additionally, the gradual red shift of the emission wavelength is related to inhomogeneous broadening or enhanced electron-phonon coupling. From Figure 3-6 (a), it is evident that the coordination field strength experienced by the Mn^{2+} ions remain unchanged. Notably, when monitoring the fluorescence decay curves of Mn^{2+} ions in samples with varying concentrations, as shown in Fig 6 (c), the decay deviates from first-order behavior as the doping concentration increases. In the initial 0–5 ms time range, the decay of Mn^{2+} ions slow down with increasing doping concentration. This suggests that even at room temperature, the sample with the lowest doping concentration (x = 1%) is still affected by thermal quenching.

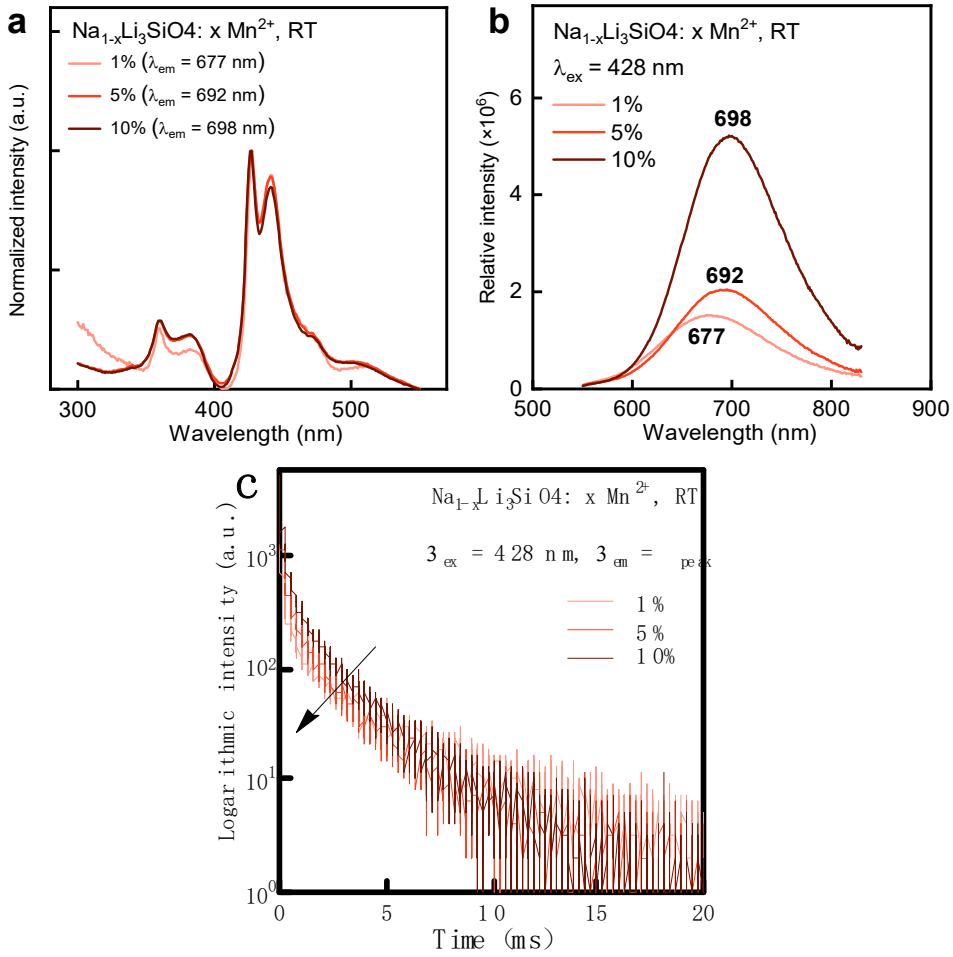

Fig. 6 The concentration-dependent excitation (a), emission (b) spectra, and lifetime decay curves (c) of the $Na_{1-x}Li_3SiO_4$: x Mn^{2+} (x = 1%, 5%, 10%) samples at room temperature.

As the Mn^{2+} doping concentration increased, the emission intensity significantly enhanced, indicating that higher doping concentrations improve luminescence efficiency. However, when the Mn^{2+} concentration exceeded 10%, emission intensity declined, possibly due to concentration quenching effects[13]. This suggests that an optimal Mn^{2+} doping ratio is crucial for optimizing the optical properties of the material. The material exhibited excellent stability under high-temperature and humid conditions, maintaining its luminescence properties over long-term storage. This characteristic makes it highly promising for applications in high-temperature operating conditions.

ISSN: 2414-1895 DOI: 10.6919/ICJE.202504_11(4).0028

4. Conclusion

In this study, a novel red luminescent material based on a $NaLi_3SiO_4$ matrix doped with Mn^{2+} was successfully synthesized, and its structural and optical characteristics were thoroughly investigated. The results indicated that the material emitted red light in the 677 nm to 698 nm range under 428 nm excitation, with enhanced emission intensity and a red-shifted peak as Mn^{2+} doping concentration increased. Additionally, the material exhibited excellent chemical stability and optical performance, making it suitable for use as an efficient red luminescent material in LED lighting and display technology. Future research will focus on optimizing doping ratios and synthesis processes to further improve luminescence efficiency and environmental stability.

References

[1] Y. Zhu, Y. Liang, S. Liu, H. Li, and J. Chen, "Narrow-Band Green-Emitting Sr_2MgAl_(22)O_(36):Mn~(2+) Phosphors with Superior Thermal Stability and Wide Color Gamut for Backlighting Display Applications," Advanced Optical Materials, vol. 7, no. 6, pp. 1801419.1-1801419.9, 2019.

[2] X.-J. Wang et al., "A novel and high brightness AlN: Mn 2+ red phosphor for field emission displays," vol. 43, no. 16, pp. 6120-6127, 2014.

[3] Q. Dong et al., "Enhanced narrow green emission and thermal stability in γ-AlON: Mn2+, Mg2+ phosphor via charge compensation," Ceramics International, vol. 45, no. 9, pp. 11868-11875, 2019.

[4] E. H. Song et al., "A thermally stable narrow-band green-emitting phosphor MgAl2O4:Mn2+for wide color gamut backlight display application," Journal of Materials Chemistry C, vol. 7, no. 27, pp. 8192-8198, 2019.

[5] H. Li et al., "Highly Efficient Green-Emitting Phosphor BaZnAl10O17:Mn~(2+) with Ultra-Narrow Band and Extremely Low Thermal Quenching for Wide Color Gamut LCD Backlights," Advanced Optical Materials, no. 24, p. 9, 2021.

[6] D. Q. Trung, N. Tu, N. V. Quang, M. T. Tran, N. V. Du, and P. T. Huy, "Non-rare-earth dual green and red-emitting Mn-doped ZnAl2O4 phosphors for potential application in plan-growth LEDs," Journal of Alloys and Compounds, vol. 845, 2020.

[7] F. Lei et al., "Photoluminescent properties of AlN: Mn2+ phosphors," Journal of Alloys and Compounds, vol. 763, pp. 466-470, 2018/09/30/ 2018.

[8] W. Wang et al., "Photoluminescence Control of UCr4C4-Type Phosphors with Superior Luminous Efficiency and High Color Purity via Controlling Site Selection of Eu2+ Activators," Chemistry of Materials, vol. 31, no. 21, pp. 9200-9210, 2019/11/12 2019.

[9] B. Nowitzki and R. Hoppe, "Neues über Oxide vom Typ A [(TO)n]: NaLi3SiO4,NaLi3GeO4 und NaLi3TiO4," (in German), Revue de chimie minérale, vol. 23, no. 2, pp. 217-230, 1986.

[10] R. Zhao, X. Guo, J. Zhang, C. Zhang, C. Deng, and R. Cui, "Optical and DFT study of a novel blue-emitting Gd7O6(BO3) (PO4)2: Bi3+ phosphor," Journal of Solid State Chemistry, vol. 324, p. 124130, 2023/08/01/ 2023.

[11] J. Xu, X. Huang, X. Cheng, M. H. Whangbo, and S. Deng, "Microscopic Mechanism of the Heat-Induced Blueshift in Phosphors and a Logarithmic Energy Dependence on the Nearest Dopant–Vacancy Distance," Angewandte Chemie International Edition, vol. 61, no. 15, 2022.

[12] Z. Liu, J. Luo, A. Yang, Z. Xie, L. He, and M. Tan, "First-principles study of the electronic structure and optical properties of Eu2+ and Mn2+-doped NaLi3SiO4 phosphor," The European Physical Journal B, vol. 97, no. 12, 2024.

[13] D. L. Dexter and J. H. Schulman, "Theory of Concentration Quenching in Inorganic Phosphors," The Journal of Chemical Physics, vol. 22, no. 6, pp. 1063-1070, 1954.